

# Coupling between a deuteron and a lattice

P L Hagelstein<sup>1</sup>, I U Chaudhary<sup>2</sup>

<sup>1</sup> Research Laboratory of Electronics, Massachusetts Institute of Technology,  
Cambridge, MA 02139, USA

E-mail: plh@mit.edu

<sup>2</sup> Department of Computer Science and Engineering, University of Engineering and  
Technology, Lahore, Pakistan

E-mail: irfanc@mit.edu

**Abstract.** We recently put forth a new fundamental lattice Hamiltonian based on an underlying picture of electrons and deuterons as elementary Dirac particles. Within this model there appears a term in which lattice vibrations are coupled to internal nuclear transitions. This is interesting as it has the potential to provide a connection between experiment and models that describe coherent energy transfer between two-level systems and an oscillator. In this work we describe a calculation of the coupling matrix element in the case of the deuteron based on the old empirical Hamada-Johnston model for the nucleon-nucleon interaction. The triplet S and D states of the the deuteron in the rest frame couples to a singlet P state through this new interaction. The singlet P state in this calculation is a virtual state with an energy of 125 MeV, and a coupling matrix element for  $z$ -directed motion given by  $2.98 \times 10^{-3} M_{Jc} \hat{P}_z$ .

## 1. Introduction

We recently obtained a new Hamiltonian for a lattice which includes interactions with internal nuclear degrees of freedom [1]. We started with a Dirac model for electrons and for nucleons on equal footing, then allowed the nuclei to be described by a finite basis expansion, and finally developed an approximation appropriate for low nuclear velocity. Our original motivation for this was to obtain a model capable of describing the mass shift associated with excited nuclear states in a configuration interaction calculation. However, the new model unexpectedly contains a new coupling term which provides for a direct interaction between lattice vibrations and nuclear transitions.

On the face of it, this new interaction term looks like it should allow for the strongly-coupled transitions that we have sought [2] in connection with the generalized lossy spin-

boson models [3, 4, 5, 6, 7, 8] that we proposed to account for some of the anomalies (such as excess heat [9, 10, 11, 12] and collimated x-ray emission [13, 14, 15, 16, 17]) that have been reported in experiments in recent years. What is needed at this point is an explicit calculation for some nuclear system to see how it works, what states are coupled to, and how big the interaction is.

In general nuclear structure models are much more complicated than atomic structure models due to the more complicated strong force interaction. We would like to work with empirical strong force models derived from scattering experiments and few-body bound state binding energies. In recent years these models have achieved impressive results [18, 19]; however, some of these strong force models involve a fair amount of work to implement. If we go back a few decades we can find simpler versions of strong force models that are easier to work with, and are sufficiently accurate to clarify the issues of interest here. In the computations that follow we will focus on the old Hamada-Johnston potential model [20]. Without question the simplest compound nucleus which should show the effects of interest is the deuteron, and so we will focus on this system in what follows.

In this formulation we have modeled the nucleons as elementary Dirac particles. As nucleons are made up of strongly interacting quarks, we know that they are not elementary Dirac particles. To do better in the case of coupling with the deuteron, we would require a description in terms of the six constituent quarks. We would expect from such a model a coupling matrix element likely somewhat different from what we calculated in this work. Even so, it makes sense here to pursue this simpler deuteron model based on simple Dirac nucleons as a step forward in the modeling process.

## 2. Basic model

In a recent paper we discussed the derivation of a finite basis approximation for a moving nucleus in the many-particle Dirac model which leads to the new coupling that we are interested in. We begin with the (relativistic) finite basis model that we obtained.

### 2.1. Finite basis approximation

In [1] we developed finite basis eigenvalue relations in the form

$$Ec_n = \sqrt{(M_n c^2)^2 + c^2 |\mathbf{P}|^2} c_n + \sum_{m \neq n} H_{nm} c_m \quad (1)$$

where the off-diagonal matrix elements were written as

$$H_{nm} = \bar{\alpha}_{nm} \cdot (c\mathbf{P}) + V_{nm} \quad (2)$$

Here  $V_{nm}$  is the relative coupling matrix element

$$V_{nm} = \left\langle \Phi_n \left| \sum_j \alpha_j \cdot c\hat{\pi}_j + \sum_j \beta_j m_j c^2 + \sum_{j < k} \hat{V}_{jk}(\boldsymbol{\xi}_k - \boldsymbol{\xi}_j) \right| \Phi_m \right\rangle \quad (3)$$

We defined  $\bar{\alpha}_{nm}$  as

$$\bar{\alpha}_{nm} = \left\langle \Phi_n \left| \sum_j \frac{m_j}{M} \alpha_j \right| \Phi_m \right\rangle \quad (4)$$

The notation for the two-body version of the problem is a bit different than what we used for the many-particle problem. It is useful to recast the relative matrix element as

$$V_{nm} = \left\langle \Phi_n \left| (\alpha_2 - \alpha_1) \cdot c\hat{\mathbf{p}} + \beta_1 m_1 c^2 + \beta_2 m_2 c^2 + \hat{V}(\mathbf{r}) \right| \Phi_m \right\rangle \quad (5)$$

The relative part of the off-diagonal matrix element corresponds to the rest frame interaction terms, which might come about from strong force interactions as in the development above for the nonrelativistic deuteron problem. What is new is the coupling with the center of mass momentum  $\mathbf{P}$  that appears in  $\bar{\alpha}_{nm} \cdot (c\mathbf{P})$ . We are interested in these new matrix elements.

### 2.2. Nonrelativistic reduction of the new interaction term

In [1] we discussed the reduction of the new interaction matrix element to the nonrelativistic case. The results can be expressed as

$$\begin{aligned}
\left\langle \Phi_f \left| \sum_j \frac{m_j}{M} \boldsymbol{\alpha}_j \cdot c\hat{\mathbf{P}} \right| \Phi_i \right\rangle &\rightarrow \frac{(E - Mc^2)}{2Mc^2} \left\langle \Phi_f \left| \sum_j \frac{\hat{\boldsymbol{\pi}}_j \cdot \hat{\mathbf{P}}}{m_j} \right| \Phi_i \right\rangle \\
&+ \frac{1}{2Mc^2} \left[ \left\langle \Phi_f \left| \sum_j (\boldsymbol{\sigma}_j \cdot c\hat{\mathbf{P}}) \left[ \frac{1}{2m_j c^2} \sum_{k < l} \hat{V}_{kl}(\boldsymbol{\xi}_l - \boldsymbol{\xi}_k) \right] (\boldsymbol{\sigma}_j \cdot c\hat{\boldsymbol{\pi}}_j) \right| \Phi_i \right\rangle \right. \\
&\left. + \left\langle \Phi_f \left| \sum_j (\boldsymbol{\sigma}_j \cdot c\hat{\boldsymbol{\pi}}_j) \left[ \frac{1}{2m_j c^2} \sum_{k < l} \hat{V}_{kl}(\boldsymbol{\xi}_l - \boldsymbol{\xi}_k) \right] (\boldsymbol{\sigma}_j \cdot c\hat{\mathbf{P}}) \right| \Phi_i \right\rangle \right] \quad (6)
\end{aligned}$$

As above, this is written for the many-particle problem, and we wish to recast it in terms of the two-body problem; we may write

$$\begin{aligned}
\left\langle \Phi_f \left| \sum_j \frac{m_j}{M} \boldsymbol{\alpha}_j \cdot c\hat{\mathbf{P}} \right| \Phi_i \right\rangle &\rightarrow \frac{(E - Mc^2)}{2Mc^2} \left( \frac{1}{m_2} - \frac{1}{m_1} \right) \left\langle \Phi_f \left| \hat{\mathbf{p}} \cdot \hat{\mathbf{P}} \right| \Phi_i \right\rangle \\
&- \frac{1}{2Mc^2} \left[ \left\langle \Phi_f \left| (\boldsymbol{\sigma}_1 \cdot c\hat{\mathbf{P}}) \left[ \frac{1}{2m_1 c^2} \hat{V}(\mathbf{r}) \right] (\boldsymbol{\sigma}_1 \cdot c\hat{\mathbf{p}}) \right| \Phi_i \right\rangle \right. \\
&\quad \left. + \left\langle \Phi_f \left| (\boldsymbol{\sigma}_1 \cdot c\hat{\mathbf{p}}) \left[ \frac{1}{2m_1 c^2} \hat{V}(\mathbf{r}) \right] (\boldsymbol{\sigma}_1 \cdot c\hat{\mathbf{P}}) \right| \Phi_i \right\rangle \right] \\
&+ \frac{1}{2Mc^2} \left[ \left\langle \Phi_f \left| (\boldsymbol{\sigma}_2 \cdot c\hat{\mathbf{P}}) \left[ \frac{1}{2m_2 c^2} \hat{V}(\mathbf{r}) \right] (\boldsymbol{\sigma}_2 \cdot c\hat{\mathbf{p}}) \right| \Phi_i \right\rangle \right. \\
&\quad \left. + \left\langle \Phi_f \left| (\boldsymbol{\sigma}_2 \cdot c\hat{\mathbf{p}}) \left[ \frac{1}{2m_2 c^2} \hat{V}(\mathbf{r}) \right] (\boldsymbol{\sigma}_2 \cdot c\hat{\mathbf{P}}) \right| \Phi_i \right\rangle \right] \quad (7)
\end{aligned}$$

### 2.3. Equal mass approximation

It is possible to split up this new interaction term into a contribution that takes the nucleon masses to be equal, and a small correction term that depends on the difference between the nucleon masses. In what follows our focus will be on the larger equal mass terms, which is equivalent to making an equal mass approximation. In this case we may write

$$\begin{aligned}
\left\langle \Phi_f \left| \sum_j \frac{m_j}{M} \boldsymbol{\alpha}_j \cdot c\hat{\mathbf{P}} \right| \Phi_i \right\rangle &\rightarrow - \left( \frac{1}{2Mc^2} \right) \left( \frac{1}{2m_{av} c^2} \right) \left[ \left\langle \Phi_f \left| (\boldsymbol{\sigma}_1 \cdot c\hat{\mathbf{P}}) \left[ \hat{V}(\mathbf{r}) \right] (\boldsymbol{\sigma}_1 \cdot c\hat{\mathbf{p}}) \right| \Phi_i \right\rangle \right. \\
&\quad \left. + \left\langle \Phi_f \left| (\boldsymbol{\sigma}_1 \cdot c\hat{\mathbf{p}}) \left[ \hat{V}(\mathbf{r}) \right] (\boldsymbol{\sigma}_1 \cdot c\hat{\mathbf{P}}) \right| \Phi_i \right\rangle \right] \\
&+ \left( \frac{1}{2Mc^2} \right) \left( \frac{1}{2m_{av} c^2} \right) \left[ \left\langle \Phi_f \left| (\boldsymbol{\sigma}_2 \cdot c\hat{\mathbf{P}}) \left[ \hat{V}(\mathbf{r}) \right] (\boldsymbol{\sigma}_2 \cdot c\hat{\mathbf{p}}) \right| \Phi_i \right\rangle \right. \\
&\quad \left. + \left\langle \Phi_f \left| (\boldsymbol{\sigma}_2 \cdot c\hat{\mathbf{p}}) \left[ \hat{V}(\mathbf{r}) \right] (\boldsymbol{\sigma}_2 \cdot c\hat{\mathbf{P}}) \right| \Phi_i \right\rangle \right] \quad (8)
\end{aligned}$$

where we have assumed that

$$m_1 = m_2 = m_{av} \quad (9)$$

In this approximation there is no longer an explicit dependence on the state energy  $E$ .

#### 2.4. Nonrelativistic approximation

It is possible to develop a nonrelativistic approximation using

$$\sqrt{(M_n c^2)^2 + c^2 |\mathbf{P}|^2} \rightarrow M_n c^2 + \frac{|\mathbf{P}|^2}{2M_n} \quad (10)$$

In this case, a finite basis model that includes center of mass dynamics to lowest order could be developed starting from a nonrelativistic Hamiltonian of the form

$$\hat{H} = \hat{M}c^2 + \frac{|\hat{\mathbf{P}}|^2}{2\hat{M}} + \frac{|\hat{\mathbf{p}}|^2}{2\mu} + \hat{V}(\mathbf{r}) + \hat{\mathbf{a}} \cdot c\hat{\mathbf{P}} \quad (11)$$

where  $\hat{M}$  is an operator that returns the rest mass energy of the nuclear state, and where  $\hat{\mathbf{a}} \cdot c\hat{\mathbf{P}}$  in the equal mass approximation is

$$\begin{aligned} \hat{\mathbf{a}} \cdot c\hat{\mathbf{P}} \rightarrow & \left( \frac{1}{2Mc^2} \right) \left( \frac{1}{2m_{av}c^2} \right) \left[ (\boldsymbol{\sigma}_2 \cdot c\hat{\mathbf{P}}) \hat{V}(\boldsymbol{\sigma}_2 \cdot c\hat{\mathbf{p}}) + (\boldsymbol{\sigma}_2 \cdot c\hat{\mathbf{p}}) \hat{V}(\boldsymbol{\sigma}_2 \cdot c\hat{\mathbf{P}}) \right. \\ & \left. - (\boldsymbol{\sigma}_1 \cdot c\hat{\mathbf{P}}) \hat{V}(\boldsymbol{\sigma}_1 \cdot c\hat{\mathbf{p}}) - (\boldsymbol{\sigma}_1 \cdot c\hat{\mathbf{p}}) \hat{V}(\boldsymbol{\sigma}_1 \cdot c\hat{\mathbf{P}}) \right] \end{aligned} \quad (12)$$

### 3. Finite-basis model for the deuteron

We know from the literature that the deuteron at rest can be modeled using a triplet S and triplet D state, since the tensor interaction mixes the two. Since the kinetic energy and potential terms preserve  $J$  and  $M_J$ , each of the triplet S states mixes with a triplet D state that has the same  $J$  and  $M_J$ .

#### 3.1. Mixing with $^1P$ states

The new interaction term causes these states to mix with singlet P states. In general, the new term does not preserve  $M_J$ , so that we would require a finite basis approximation that distinguishes the different sublevels. However, it is possible to focus on a special case of the new interaction which does preserve  $M_J$ . This occurs if we restrict our attention to

$$\hat{\mathbf{P}} = \hat{\mathbf{i}}_z \hat{P}_z \quad (13)$$

We find in this case that mixing occurs for  $|M_J| = 1$ , but not for  $M_J = 0$ . In response, we might write

$$\Psi = \Psi_{3S} + \Psi_{3D} + \Psi_{1P} \quad (14)$$

with the understanding that

$$\Psi_{1P}(J_M = 0) \rightarrow 0 \quad (15)$$

#### 3.2. Basis state construction

Nuclear state construction is usually carried out in the isospin scheme, with antisymmetry enforced through the application of the generalized Pauli principle. The two-body problem is particularly simple in this regard, with spin, isospin and spatial components restricted to being either symmetric ( $s$ ) or antisymmetric ( $a$ ); we may write for the three states

$$\Psi_{3S} = R(s)S(s)T(a) \quad (16)$$

$$\Psi_{3D} = R(s)S(s)T(a) \quad (17)$$

$$\Psi_{1P} = R(a)S(a)T(a) \quad (18)$$

The antisymmetric spin and isospin terms  $S(a)$  and  $T(a)$  are singlets, and the symmetric spin and isospin terms  $S(s)$  and  $T(s)$  are triplets.

### 3.3. Triplet S state

The S state is a triplet spin state, so we may write it as

$$\begin{aligned}\Psi_{3S} &= \Psi_{3S}(S = 1, M_S; T = 0, M_T = 0; l = 0, m = 0) \\ &= \frac{u(r)}{r} Y_{00}(\theta, \phi) |1, M_S\rangle_S |0, 0\rangle_T\end{aligned}\quad (19)$$

The  $Y_{lm}(\theta, \phi)$  are spherical harmonics; we choose  $l = 0$  and  $m = 0$  since we are working with an S state. The  $|S, M_S\rangle_S$  are spin functions for the neutron and proton spins; the  $|T, M_T\rangle_T$  are isospin functions, and we have used an isospin singlet function here.

### 3.4. Triplet D state

We can develop a D state by applying the tensor  $\hat{S}_{12}$  operator on an S state. This approach was used early on as a convenient way of generating few-body wavefunctions for variational calculations in nuclear physics. We may write

$$\Psi_{3D} = \frac{1}{\sqrt{8}} \hat{S}_{12} \left[ \frac{v(r)}{r} Y_{00}(\theta, \phi) |1, M_S\rangle_S |0, 0\rangle_T \right] \quad (20)$$

This construction is convenient since

$$\hat{S}_{12} \Psi_{3D} = \sqrt{8} \left[ \frac{v(r)}{r} Y_{00}(\theta, \phi) |1, M_S\rangle_S |0, 0\rangle_T \right] - 2\Psi_{3D} \quad (21)$$

### 3.5. Singlet P state

The singlet P state for a particular calculation can be specified using

$$\begin{aligned}\Psi_{1P} &= \Psi_{1P}(S = 0, M_S = 0; T = 0, M_T = 0; l = 1, m) \\ &= i \frac{w(r)}{r} Y_{1m}(\theta, \phi) |0, 0\rangle_S |0, 0\rangle_T\end{aligned}\quad (22)$$

Including an  $i$  here leads to real coupling coefficients in what follows.

### 3.6. Normalization

We can evaluate the normalization integral for these states simply; we write

$$\begin{aligned}\langle \Psi | \Psi \rangle &= \langle \Psi_{3S} | \Psi_{3S} \rangle + \langle \Psi_{3D} | \Psi_{3D} \rangle + \langle \Psi_{1P} | \Psi_{1P} \rangle \\ &= \int_0^\infty |u(r)|^2 + |v(r)|^2 + |w(r)|^2 dr\end{aligned}\quad (23)$$

### 3.7. Expectation value of Hamiltonian terms

We are interested in developing coupled channel equations that include the new interaction. For the problem in the rest frame, this is most easily accomplished by developing an expression for the total energy and then using the variational principle. We can use the same basic approach here for the moving frame version of the problem. We begin with

$$\begin{aligned}
\left\langle \Psi \left| \frac{\mathbf{p}^2}{2\mu} + \hat{V} + (\mathbf{a} \cdot c\hat{\mathbf{P}})_z \right| \Psi \right\rangle = & \\
& \left\langle \Psi_{3S} \left| \frac{\mathbf{p}^2}{2\mu} + \hat{V} \right| \Psi_{3S} \right\rangle + \left\langle \Psi_{3D} \left| \frac{\mathbf{p}^2}{2\mu} + \hat{V} \right| \Psi_{3D} \right\rangle + \left\langle \Psi_{1P} \left| \frac{\mathbf{p}^2}{2\mu} + \hat{V} \right| \Psi_{1P} \right\rangle \\
& + \left\langle \Psi_{3S} \left| \hat{V} \right| \Psi_{3D} \right\rangle + \left\langle \Psi_{3D} \left| \hat{V} \right| \Psi_{1S} \right\rangle + \left\langle \Psi_{1P} \left| (\mathbf{a} \cdot c\hat{\mathbf{P}})_z \right| \Psi_{1S} \right\rangle \\
& + \left\langle \Psi_{1P} \left| (\mathbf{a} \cdot c\hat{\mathbf{P}})_z \right| \Psi_{3D} \right\rangle + \left\langle \Psi_{3S} \left| (\mathbf{a} \cdot c\hat{\mathbf{P}})_z \right| \Psi_{1P} \right\rangle + \left\langle \Psi_{3D} \left| (\mathbf{a} \cdot c\hat{\mathbf{P}})_z \right| \Psi_{1P} \right\rangle \quad (24)
\end{aligned}$$

### 3.8. Diagonal matrix elements

We can evaluate the diagonal matrix elements directly using Mathematica to obtain

$$\left\langle \Psi_{3S} \left| \frac{\mathbf{p}^2}{2\mu} + \hat{V} \right| \Psi_{3S} \right\rangle = \int_0^\infty u(r) \left[ -\frac{\hbar^2}{2\mu} \frac{d^2}{dr^2} - 3v_C^{et}(r) \right] u(r) dr \quad (25)$$

$$\left\langle \Psi_{3D} \left| \frac{\mathbf{p}^2}{2\mu} + \hat{V} \right| \Psi_{3D} \right\rangle = \int_0^\infty v(r) \left[ -\frac{\hbar^2}{2\mu} \frac{d^2}{dr^2} - 3v_C^{et}(r) + 6v_T^{et}(r) - 3v_{LS}^{et}(r) - 3v_{LL}^{et}(r) \right] v(r) dr \quad (26)$$

$$\left\langle \Psi_{1P} \left| \frac{\mathbf{p}^2}{2\mu} + \hat{V} \right| \Psi_{1P} \right\rangle = \int_0^\infty w(r) \left[ -\frac{\hbar^2}{2\mu} \frac{d^2}{dr^2} + 9v_C^{os}(r) - 2v_{LL}^{os}(r) \right] w(r) dr \quad (27)$$

### 3.9. Off-diagonal potential matrix elements

In the case of the Hamada-Johnston potential, there occur off-diagonal matrix elements between the triplet S and singlet D states, which are given by

$$\left\langle \Psi_{3S} \left| \hat{V} \right| \Psi_{3D} \right\rangle = \left\langle \Psi_{3D} \left| \hat{V} \right| \Psi_{3S} \right\rangle = -3\sqrt{8} \int_0^\infty u(r) v_T^{et}(r) v(r) dr \quad (28)$$

The superscript *et* in the associated potentials here is connected with the even triplet channel, since the Hamada-Johnston potentials are fit for the different channels separately.



## 3.10. Off-diagonal matrix elements for the new interaction

For the off-diagonal matrix elements of the new interaction, we have used Mathematica to compute

$$\begin{aligned}
\langle \Phi_{1P} | (\mathbf{a} \cdot c\hat{\mathbf{P}})_z | \Phi_{3S} \rangle &= M_J \left( \frac{1}{2Mc^2} \right) \left( \frac{1}{2m_{av}c^2} \right) (\hbar c)(c\hat{P}_z) \\
&\quad \left\{ -2\sqrt{3} \int_0^\infty w(r) \left[ \frac{d}{dr} v_C^{eT}(r) \right] u(r) dr \right. \\
&\quad + 12\sqrt{3} \int_0^\infty w(r) v_T^{eT}(r) \left[ \frac{d}{dr} u(r) + \frac{u(r)}{r} \right] dr \\
&\quad + 8\sqrt{3} \int_0^\infty w(r) \left[ \frac{d}{dr} v_T^{eT}(r) \right] u(r) dr \\
&\quad + \frac{2}{\sqrt{3}} \int_0^\infty w(r) v_{LS}^{eT}(r) \left[ \frac{d}{dr} u(r) - \frac{u(r)}{r} \right] dr \\
&\quad \left. - 2\sqrt{3} \int_0^\infty w(r) v_{LL}^{eT}(r) \left[ \frac{d}{dr} u(r) - \frac{u(r)}{r} \right] dr \right\} \tag{29}
\end{aligned}$$

$$\begin{aligned}
\langle \Phi_{1P} | (\mathbf{a} \cdot c\hat{\mathbf{P}})_z | \Phi_{3D} \rangle &= M_J \left( \frac{1}{2Mc^2} \right) \left( \frac{1}{2m_{av}c^2} \right) (\hbar c)(c\hat{P}_z) \\
&\quad \left\{ -\sqrt{6} \int_0^\infty w(r) \left[ \frac{d}{dr} v_C^{eT}(r) \right] v(r) dr \right. \\
&\quad + 6\sqrt{6} \int_0^\infty w(r) v_T^{eT}(r) \left[ \frac{d}{dr} v(r) + \frac{v(r)}{r} \right] dr \\
&\quad + 4\sqrt{6} \int_0^\infty w(r) \left[ \frac{d}{dr} v_T^{eT}(r) \right] v(r) dr \\
&\quad - \sqrt{\frac{8}{3}} \int_0^\infty w(r) v_{LS}^{eT}(r) \left[ \frac{d}{dr} v(r) + 2\frac{v(r)}{r} \right] dr \\
&\quad - \sqrt{6} \int_0^\infty w(r) \left[ \frac{d}{dr} v_{LS}^{eT}(r) \right] v(r) dr \\
&\quad - 2\sqrt{6} \int_0^\infty w(r) v_{LL}^{eT}(r) \left[ \frac{d}{dr} v(r) + 2\frac{v(r)}{r} \right] dr \\
&\quad \left. - \sqrt{6} \int_0^\infty w(r) \left[ \frac{d}{dr} v_{LL}^{eT}(r) \right] v(r) dr \right\} \tag{30}
\end{aligned}$$

$$\langle \Phi_{3S} | (\mathbf{a} \cdot c\hat{\mathbf{P}})_z | \Phi_{1P} \rangle = M_J \left( \frac{1}{2Mc^2} \right) \left( \frac{1}{2m_{av}c^2} \right) (\hbar c)(c\hat{P}_z)$$

$$\begin{aligned}
& \left\{ -2\sqrt{3} \int_0^\infty u(r) \left[ \frac{d}{dr} v_C^{eT}(r) \right] w(r) dr \right. \\
& + 12\sqrt{3} \int_0^\infty u(r) v_T^{eT}(r) \left[ -\frac{d}{dr} w(r) + \frac{w(r)}{r} \right] dr \\
& - 4\sqrt{3} \int_0^\infty u(r) \left[ \frac{d}{dr} v_T^{eT}(r) \right] w(r) dr \\
& + \frac{2}{\sqrt{3}} \int_0^\infty w(r) v_{LS}^{eT}(r) \left[ -\frac{d}{dr} u(r) - \frac{u(r)}{r} \right] dr \\
& - \frac{2}{\sqrt{3}} \int_0^\infty u(r) \left[ \frac{d}{dr} v_{LS}^{eT}(r) \right] w(r) dr \\
& - 2\sqrt{3} \int_0^\infty w(r) v_{LL}^{eT}(r) \left[ -\frac{d}{dr} u(r) - \frac{u(r)}{r} \right] dr \\
& \left. + 2\sqrt{3} \int_0^\infty u(r) \left[ \frac{d}{dr} v_{LL}^{eT}(r) \right] w(r) dr \right\} \tag{31}
\end{aligned}$$

$$\begin{aligned}
\langle \Phi_{3D} | (\mathbf{a} \cdot c\hat{\mathbf{P}})_z | \Phi_{1P} \rangle &= M_J \left( \frac{1}{2Mc^2} \right) \left( \frac{1}{2m_{av}c^2} \right) (\hbar c) (c\hat{P}_z) \\
& \left\{ -\sqrt{6} \int_0^\infty v(r) \left[ \frac{d}{dr} v_C^{eT}(r) \right] 2(r) dr \right. \\
& + 6\sqrt{6} \int_0^\infty v(r) v_T^{eT}(r) \left[ -\frac{d}{dr} w(r) + \frac{w(r)}{r} \right] dr \\
& - 2\sqrt{6} \int_0^\infty v(r) \left[ \frac{d}{dr} v_T^{eT}(r) \right] w(r) dr \\
& - \sqrt{\frac{8}{3}} \int_0^\infty w(r) v_{LS}^{eT}(r) \left[ -\frac{d}{dr} v(r) + 2\frac{v(r)}{r} \right] dr \\
& - \sqrt{\frac{2}{3}} \int_0^\infty w(r) \left[ \frac{d}{dr} v_{LS}^{eT}(r) \right] v(r) dr \\
& - 2\sqrt{6} \int_0^\infty w(r) v_{LL}^{eT}(r) \left[ -\frac{d}{dr} v(r) + 2\frac{v(r)}{r} \right] dr \\
& \left. + \sqrt{6} \int_0^\infty w(r) \left[ \frac{d}{dr} v_{LL}^{eT}(r) \right] v(r) dr \right\} \tag{32}
\end{aligned}$$

#### 4. Coupled-channel equations

We have specified a finite basis problem with three channels, which would produce three complicated coupled-channel equations if we decided to treat the different basis states on equal footing. However, since the momentum  $\mathbf{P}$  that we are interested in for applications of this model is small, the triplet S and D channels are then best considered to constitute the unperturbed deuteron problem, and the singlet P channel will contain the weak response of the deuteron to the  $\mathbf{a} \cdot c\mathbf{P}$  perturbation.

In this case, it seems appropriate to develop the coupled triplet S and D channels consistent with the rest frame deuteron problem. Once the associated wavefunctions are known, then we can use them to approximate the occupation of the singlet P channel.

##### 4.1. Rarita-Schwinger equations

Given the approach outlined above, we can optimize the channel wavefunctions  $u(r)$  and  $v(r)$  by minimizing the rest frame energy

$$\begin{aligned} & \left\langle \Psi_{3S} \left| \frac{\mathbf{p}^2}{2\mu} + \hat{V} \right| \Psi_{3S} \right\rangle + \left\langle \Psi_{3D} \left| \frac{\mathbf{p}^2}{2\mu} + \hat{V} \right| \Psi_{3D} \right\rangle + \left\langle \Psi_{3S} \left| \hat{V} \right| \Psi_{3D} \right\rangle + \left\langle \Psi_{3D} \left| \hat{V} \right| \Psi_{3S} \right\rangle = \\ & \int_0^\infty u(r) \left[ -\frac{\hbar^2}{2\mu} \frac{d^2}{dr^2} - 3v_C^{et}(r) \right] u(r) dr \\ & + \int_0^\infty v(r) \left[ -\frac{\hbar^2}{2\mu} \frac{d^2}{dr^2} + \frac{6\hbar^2}{2\mu r^2} - 3v_C^{et}(r) + 6v_T^{et}(r) - 3v_{LS}^{et}(r) - 3v_{LL}^{et}(r) \right] v(r) dr \\ & - 6\sqrt{8} \int_0^\infty u(r) v_T^{et}(r) v(r) dr \end{aligned} \quad (33)$$

The minimization of this rest frame energy leads to the constraints

$$E_r u(r) = \left[ -\frac{\hbar^2}{2\mu} \frac{d^2}{dr^2} - 3v_C^{et}(r) \right] u(r) + \left[ -3\sqrt{8}v_T^{et}(r) \right] v(r) \quad (34)$$

$$\begin{aligned} E_r v(r) = & \left[ -\frac{\hbar^2}{2\mu} \frac{d^2}{dr^2} + \frac{6\hbar^2}{2\mu r^2} - 3v_C^{et}(r) + 6v_T^{et}(r) - 3v_{LS}^{et}(r) - 3v_{LL}^{et}(r) \right] v(r) \\ & + \left[ -3\sqrt{8}v_T^{et}(r) \right] u(r) \end{aligned} \quad (35)$$

where  $E_r$  is the relative energy. We recognize these as the Rarita-Schwinger equations based on the Hamada-Johnston potential model.

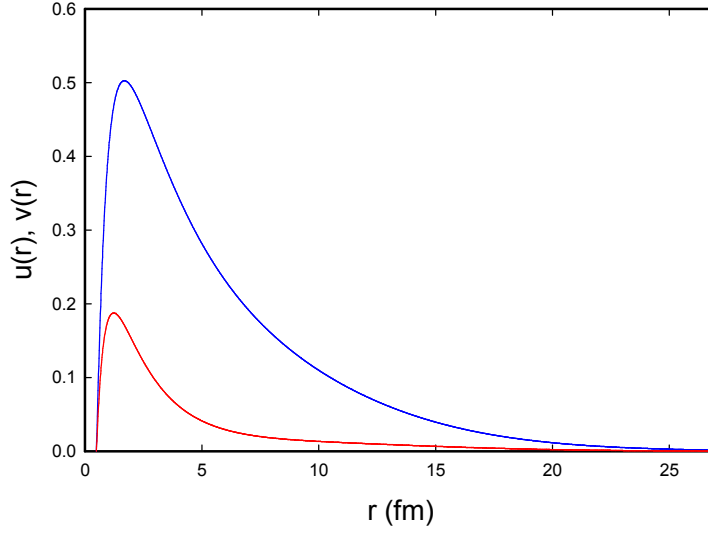


**Figure 1.** Numerical solutions of the Rarita-Schwinger equations for the deuteron using the Hamada-Johnston potential. The solution for the S state [ $u(r)$ ] is shown in blue; the solution for the D state [ $v(r)$ ] is shown in red.

#### 4.2. Rest frame triplet S and D channel wavefunctions

We have solved the Rarita-Schwinger equations to obtain the channel wavefunctions plotted in Figure 1. The triplet S channel wavefunction  $u(r)$  is larger and extends out to a relatively large radial separation, and the triplet D channel wavefunction  $v(r)$  is smaller and localized to much smaller radial separation. We can see the effect of the hard core potential in the zero boundary condition at the cut off radius.

#### 4.3. Optimization of the singlet P channel

In the perturbation theory approach outlined above, we can approximate the occupation of the singlet P channel in terms of known triple S and D channel wavefunctions. The associated constraint on the channel wavefunction can be written as

$$\begin{aligned} \left[ -\frac{\hbar^2}{2\mu} \frac{d^2}{dr^2} + \frac{2\hbar^2}{2\mu r^2} + 9v_C^{os}(r) - 2v_{LL}^{os}(r) \right] w(r) &= M_J \left( \frac{1}{2Mc^2} \right) \left( \frac{1}{2m_{av}c^2} \right) (\hbar c)(c\hat{P}_z) \\ &\times \left\{ -2\sqrt{3} \left[ \frac{d}{dr} v_C^{eT}(r) \right] u(r) + 12\sqrt{3} v_T^{eT}(r) \left[ \frac{d}{dr} u(r) + \frac{u(r)}{r} \right] + 8\sqrt{3} \left[ \frac{d}{dr} v_T^{eT}(r) \right] u(r) \right. \\ &\quad \left. + \frac{2}{\sqrt{3}} v_{LS}^{eT}(r) \left[ \frac{d}{dr} u(r) - \frac{u(r)}{r} \right] - 2\sqrt{3} v_{LL}^{eT}(r) \left[ \frac{d}{dr} u(r) - \frac{u(r)}{r} \right] \right\} \end{aligned}$$

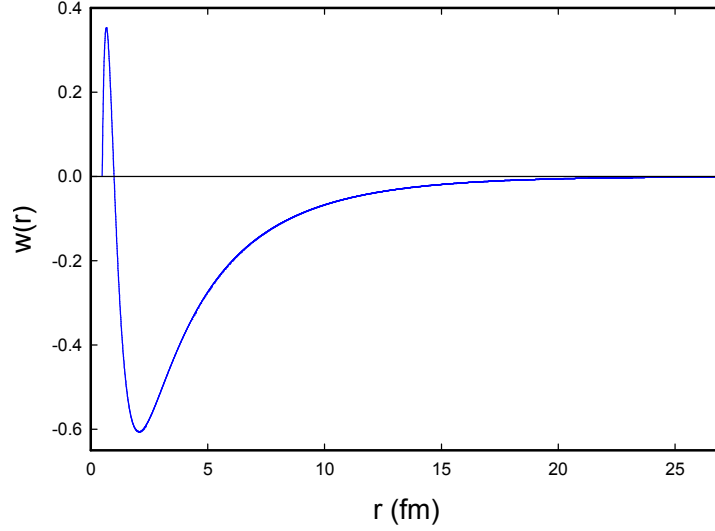


**Figure 2.** Numerical solution for the normalized singlet P radial wavefunction.

$$\begin{aligned}
& +M_J \left( \frac{1}{2Mc^2} \right) \left( \frac{1}{2m_{av}c^2} \right) (\hbar c)(c\hat{P}_z) \left\{ -\sqrt{6} \left[ \frac{d}{dr} v_C^{eT}(r) \right] v(r) \right. \\
& +6\sqrt{6} v_T^{eT}(r) \left[ \frac{d}{dr} v(r) + \frac{v(r)}{r} \right] + 4\sqrt{6} \left[ \frac{d}{dr} v_T^{eT}(r) \right] v(r) - \sqrt{\frac{8}{3}} v_{LS}^{eT}(r) \left[ \frac{d}{dr} v(r) + 2\frac{v(r)}{r} \right] \\
& \left. -\sqrt{6} \left[ \frac{d}{dr} v_{LS}^{eT}(r) \right] v(r) - 2\sqrt{6} v_{LL}^{eT}(r) \left[ \frac{d}{dr} v(r) + 2\frac{v(r)}{r} \right] - \sqrt{6} \left[ \frac{d}{dr} v_{LL}^{eT}(r) \right] v(r) \right\} \quad (36)
\end{aligned}$$

We have solved this equation numerically assuming that  $u(r)$  and  $v(r)$  are fixed solutions of the Rarita-Schwinger equations, and the resulting normalized solution for  $w(r)$  is shown in Figure 2.

#### 4.4. Equivalent two-level model parameters

From the computation outlined above we can derive an equivalent two-level system model in the form

$$E \begin{pmatrix} c_1 \\ c_2 \end{pmatrix} = \begin{pmatrix} H_{11} & H_{12} \\ H_{21} & H_{22} \end{pmatrix} \begin{pmatrix} c_1 \\ c_2 \end{pmatrix} \quad (37)$$

We compute

$$H_{11} = -2.245 \text{ MeV} \quad (38)$$

$$H_{22} = 125.4 \text{ MeV} \quad (39)$$

$$H_{12} = H_{21} = 2.98 \times 10^{-3} M_J(c\hat{P}_z) \quad (40)$$

The off-diagonal coupling matrix elements are somewhat smaller than we were hoping for, and future work will be needed to understand if this coupling is sufficiently large to account for experimental results. In addition, we have found that these off-diagonal matrix element depend on the nuclear spin, which suggests that the system may respond to net spin alignment.

## 5. Discussion and conclusions

We recently proposed a new fundamental Hamiltonian for condensed matter lattice problems that includes coupling to nuclear internal degrees of freedom. From our perspective this new coupling seems to be what is needed to account for the excess heat effect in the Fleischmann-Pons experiment. What has been needed in order to evaluate the models that result is an estimate for the coupling matrix element.

The development of an estimate for this matrix element is challenging for a variety of reasons. We have presumed in the derivation of the fundamental Hamiltonian that it is sufficient to model the nucleons as elementary Dirac particles. However, we know that nucleons are composite particles made up of quarks and gluons, and that it is unlikely that using a Dirac model as we have done is going to give accurate results. To do better we probably need to go back and develop a better fundamental Hamiltonian based on quarks and electrons. If it is possible to obtain reasonable nucleon models from empirical potentials, then we may be able to develop a better estimate for the deuteron coupling matrix element. Working directly with bound state QCD at this stage does not seem to be an attractive option.

Once we have decided on the simpler model that adopts an elementary Dirac particle model for nucleons, then it is an issue of whether to use a relativistic or nonrelativistic model, and further it is an issue of what potential to use. Since these computations involve a fair amount of work, it seemed sensible to adopt a nonrelativistic model since it is simpler, and to work with an older relatively simple nuclear model. The Hamada-Johnston potential fits the bill in this regard, as it is sufficiently simple that we are able to complete a calculation in relatively short order. Perhaps the most work in this computation was the evaluation of the spin, isospin, and angular momentum algebra; for this we relied on brute force Mathematica calculations.

In the end, we have developed a model for the coupling between the different nuclear spin states of the ground state deuteron and lattice-induced coupling to a highly-excited singlet P virtual state. The energy of this virtual state is about 125 MeV in this model, which is consistent with our expectations. The coupling matrix element fell short of what we had hoped for by about an order of magnitude. We will need to clarify in future calculations if this is sufficiently large to be relevant to experimental results.

The coupling matrix element in this model is proportional to  $M_J$ , which is interesting in connection with the reported dependence of excess heat on the strength of an applied magnetic field. Since the matrix element is proportional to  $M_J$ , there is the

potential for a larger coupling if the deuteron spins can be aligned. We are interested in pursuing this possibility in future work.



## References

- [1] P. L. Hagelstein and I. U. Chaudhary, "Including nuclear degrees of freedom in a lattice Hamiltonian," *J. Cond. Mat. Nucl. Sci.* (in press).
- [2] P. L. Hagelstein, "Bird's eye view of phonon exchange models for excess heat in the Fleischmann-Pons experiment," *J. Cond. Mat. Nucl. Sci.* (in press).
- [3] P. L. Hagelstein and I. U. Chaudhary, "Energy exchange in the lossy spin-boson model," *J. Cond. Mat. Nucl. Sci.* **5** (2011) 52.
- [4] P. L. Hagelstein and I. U. Chaudhary, "Second-order formulation and scaling in the lossy spin-boson model," *J. Cond. Mat. Nucl. Sci.* **5** (2011) 87.
- [5] P. L. Hagelstein and I. U. Chaudhary, "Local approximation for the lossy spin-boson model," *J. Cond. Mat. Nucl. Sci.* **5** (2011) 102.
- [6] P. L. Hagelstein and I. U. Chaudhary, "Coherent energy exchange in strong coupling limit of the lossy spin-boson model," *J. Cond. Mat. Nucl. Sci.* **5** (2011) 116.
- [7] P. L. Hagelstein and I. U. Chaudhary, "Generalization of the lossy spin-boson model to donor and receiver systems," *J. Cond. Mat. Nucl. Sci.* **5** (2011) 140.
- [8] P. L. Hagelstein and I. U. Chaudhary, "Errata and comments on a recent set of papers in Journal of Condensed Matter Nuclear Science," *J. Cond. Mat. Nucl. Sci.* (in press).
- [9] M. Fleischmann, S. Pons and M. Hawkins, *J. Electroanal. Chem.*, **201**, (1989) 301; errata, **263** (1990) 187.
- [10] M. Fleischmann, S. Pons, M.W. Anderson, L.J. Li and M. Hawkins, *J. Electroanal. Chem.*, **287** (1990) 293.
- [11] M. C. H. McKubre, S. Crouch-Baker, R. C. Rocha-Filho, S. I. Smedley, F. L. Tanzella, T. O. Passell, J. Santucci, *J. Electroanal. Chem.* **368** (1994) 55.
- [12] E. Storms, *Science of Low Energy Nuclear Reaction: A comprehensive compilation of evidence and explanations about cold fusion*, World Scientific Publishing Co, Singapore (2007).
- [13] A. B. Karabut, "X-ray emission in the high-current glow discharge experiments," *Condensed Matter Nuclear Science, Proc. ICCF9*, edited by Xing Z. Li, p. 155 (2002).
- [14] A. B. Karabut and S. A. Kolomeychenko, "Experiments characterizing the x-ray emission from a solid-state cathode using a high-current glow discharge," *Condensed Matter Nuclear Science, Proc. ICCF10*, edited by P. L. Hagelstein and S. R. Chubb, p. 585 (2003).
- [15] A. B. Karabut, "Research into characteristics of x-ray emission laser beams from solid state cathode medium of high-current glow discharge," *Condensed Matter Nuclear Science, Proc. ICCF11*, edited by J. P. Biberian, p. 253 (2004).
- [16] A. B. Karabut, "Study of energetic and temporal characteristics of x-ray emission from solid state cathode medium of high-current glow discharge," *Condensed Matter Nuclear Science, Proc. ICCF12*, edited by A. Takahashi, K.-I. Ota, and Y. Iwamura, p. 344 (2005).
- [17] A. B. Karabut, E. A. Karabut, P. L. Hagelstein, "Spectral and temporal characteristics of x-ray emission from metal electrodes in a high-current glow discharge," *J. Cond. Mat. Nucl. Sci.* (in press).
- [18] H. Kamada, A. Nogga, W. Glöckle, E. Hiyama, M. Kamimura, K. Varga, Y. Suzuki, M. Viviani, A. Kievsky, and S. Rosati, "Benchmark test calculation of a four-nucleon bound state," *Phys. Rev. C* **64** (2001) 044001.

- [19] R. Machleidt and D. R. Entem, “Chiral effective field theory and nuclear forces,” *Physics Reports* **503** (2011) 1.
- [20] T. Hamada and I. D. Johnston, “A potential model representation of two-nucleon data below 315 MeV,” *Nucl. Phys.* **34** (1962) 382.